Thermodynamic properties of liquid Rb-Pb alloys

1990 J. Phys.: Condens. Matter 2 209

(http://iopscience.iop.org/0953-8984/2/1/017)

J. Phys.: Condens. Matter **2** (1990) 209–220. Printed in the UK

Thermodynamic properties of liquid Rb–Pb alloys

P J Tumidajski†‡, A Petric†§, T Takenaka†‖, A D Pelton¶ and Marie-Louise Saboungi†

† Chemical Technology Division/Materials Science Program, Argonne National Laboratory, Argonne, Illinois 60439-4837, USA

¶ Centre de Recherche en Calcul Thermochimique, Ecole Polytechnique, Montreal, Quebec, Canada H3C 3A7

Received 12 June 1989, in final form 29 August 1989

Abstract. Thermodynamic properties of liquid Rb–Pb alloys are deduced from electromotive force measurements using a coulometric titration technique. From a combination of measurements as a function of composition or temperature, Gibbs energies of mixing, entropies of mixing, and excess heat capacities are derived for alloy compositions covering the range from pure lead to 70 at.% Rb. At the equiatomic composition, extrema are obtained in the variations with composition of the Darken excess stability, the entropy, and the excess heat capacity. Recent electrical resistivity, calorimetric, and neutron diffraction measurements indicated an unusual behaviour at the same composition, which was interpreted in terms of polyanionic species. Our results corroborate the presence of structural units that become predominant at the equiatomic composition. A departure from this composition through addition of Rb or Pb leads to a decrease and dissociation of these species into free atoms.

1. Introduction

The interpretation of the thermodynamic behaviour of liquid alkali metal–lead alloys has presented many challenges. These alloys have unusual properties in the liquid state, e.g. the electrical, optical, magnetic, and thermodynamic properties change sharply at the equiatomic (1:1) and/or the 'octet' (4:1) composition. There have been several thermodynamic studies on the Li–Pb, Na–Pb, and K–Pb alloy systems [1–9]. Studies of Li–Pb alloys by Saboungi *et al* [2] indicated an ordering in the alloy with a maximum at the stoichiometric Li_4Pb composition. Thermodynamic measurements of Na–Pb alloys revealed the presence of two peaks in the excess stability and the excess heat capacity at the NaPb and Na_4Pb compositions [3–5].

The K–Pb system differs from Na–Pb and Li–Pb because all thermodynamic functions, including excess stabilities and heat capacities, have unusual behaviour only

‡ Present address: University of Western Ontario, Department of Materials Engineering, London, Ontario, Canada N6A 5B9.

§ Present address: McMaster University, Department of Materials Science and Engineering, Hamilton, Ontario, Canada L8S 4L7.

‖ Present address: Research Institute of Mineral Dressing and Metallurgy, Tohoku University, Katahira-cho, Sendai 980, Japan.

0953-8984/90/010209 + 12 $03.50

around the equiatomic composition [7] and not at the 'octet' composition. Furthermore, at the (1 : 1) composition the excess heat capacity is very large, and exhibits a pronounced temperature dependence [8]. Recent calorimetric experiments indicate a large heat capacity anomaly for RbPb alloys [9]. Electrical resistivity measurements for alkali–lead alloys have shown maxima at either the octet and/or the equiatomic composition [10]. The variations of the electrical resistivity with composition for K–Pb alloys are different from Li–Pb and Na–Pb alloys because only one maximum at the equiatomic composition KPb is reported, compared with maxima at Li_4Pb for Li–Pb and at Na_4Pb and NaPb for Na–Pb [10]. A maximum was observed in the electrical resistivity of Rb–Pb alloys at the equiatomic composition and a large negative temperature coefficient [10–11]. According to the Mott and Davis classification, RbPb and KPb belong to regime II where the conductivity is between $\simeq 3000$ and $\simeq 300\ \Omega^{-1}\ cm^{-1}$ and the interatomic distance is very close to the mean free path.

Because anomalies in electrical properties generally appear to parallel closely anomalies in thermodynamic properties, it is of interest to investigate systematically the thermodynamic properties of liquid alkali–Pb alloys. In this paper, we report the composition and temperature dependence of the activity coefficient of rubidium in liquid Rb–Pb alloys, as well as the entropy and heat capacity. These functions were derived from electromotive force measurements carried out with a coulometric titration technique using a solid electrolyte (rubidium substituted β''-alumina) over a temperature interval of 610–910 K and for compositions ranging from pure lead to 70% Rb.

It should be noted that, to our knowledge, this is the only investigation of the composition dependence of the thermodynamic properties of liquid Rb–Pb alloys. The lack of information is due to a combination of chemical 'aggressivity' of this alloy, as well as the paucity of experimental techniques for handling such materials. Only recently was rubidium-substituted β''-alumina demonstrated to be usable as a solid electrolyte for coulometric titration experiments [12]. Vapour pressure measurements cannot give the needed accuracy to examine in detail the behaviour of thermodynamic functions and the evaluation of heat capacities.

2. Experimental procedure

The experimental apparatus used for the electromotive force measurements has been described earlier [7]. Briefly, the electrochemical cell consisted of two half-cells, a secondary reference electrode (RE) half-cell, and a working electrode (WE) half-cell, represented schematically as

$$\text{Bi–3 at.\% Rb//Rb } \beta''\text{–}Al_2O_3\text{//Bi–2 at.\% Rb//Rb } \beta''\text{–}Al_2O_3\text{//Pb–Rb.} \qquad \text{(I)}$$

The secondary reference electrode half-cell consisted of a Bi–3 at.% Rb alloy contained in a hermetically sealed Rb substituted β''-alumina tube; this composition was chosen to reduce the Rb activity and, thus, its vapour pressure. The WE consisted of a Rb–Pb alloy in a Rb–β''-alumina tube sealed in the same fashion. The composition of the WE was accurately varied by coulometric titration. Both half-cells were immersed to the same depth in a stirred Bi–2 at.% Rb bath contained in a molybdenum crucible. Its function was to provide electrical contact, and to serve as a source and sink of Rb during

coulometric titration. The secondary RE was calibrated against a pure Rb-electrode using a cell schematically given as

$$\text{Rb}//\text{Rb}\ \beta''\text{–Al}_2\text{O}_3//\text{Bi–2 at.\% Rb}//\text{Rb}\ \beta''\text{–Al}_2\text{O}_3//\text{Bi–3 at.\% Rb}. \quad \text{(II)}$$

All subsequent EMFs are reported relative to the pure liquid Rb reference electrode.

Cells were loaded inside a high purity He glovebox. Accurately weighed amounts of high purity filtered Pb were loaded into the cell in small pieces; rubidium was generated by coulometric titration that involved the application of a potential across the electrolyte between the WE and the counter electrode. At the temperatures of the experiments, there is negligible electronic transport through the solid electrolyte. Consequently, exactly one mole of Rb will be transported for each Faraday of charge. Compositional changes can be controlled down to the ppm range. Additionally, the introduction of oxides or impurity ions is avoided.

High purity Pb (99.999%) and rubidium† (99.85%) were used. The major impurity in the Rb was 0.1 at.% Cs. The fabrication and sealing procedures for the Rb–β''-alumina have been described in detail elsewhere [7]. Temperatures measured with a calibrated (Pt and Pt–10 at.% Rh) thermocouple immersed in the molybdenum crucible were stable to less than ±1 K.

3. Results and discussion

Several independent experiments were carried out to observe the variation of EMF with composition and temperature. Two cells were operated isothermally at 878 K to determine the compositional dependence of the EMF from 0 to 70 at.% Rb. In addition, two independent experiments were performed at 673 K and 878 K in the dilute solution range to test the Henrian behaviour of the Rb–Pb solutions. Finally, the isopleth temperature dependence of EMFs from 10 at.% to 60 at.% Rb was determined.

All cell EMFs were stable and reproducible to within ±1–2 mV. Coulometric titrations were, in all cases, performed with overpotentials of less than 500 mV. Cell lifetimes varied according to Rb composition and thermal treatment. In general, cells of dilute compositions (<30 at.% Rb) lasted for more than a week. However, for cells of high Rb content (>45 at.% Rb), and for those cells that were thermally cycled, lifetimes were of the order of two to three days.

3.1. Nernst behaviour and thermodynamic functions

The overall spontaneous reaction for the Rb concentration cell is

$$\text{Rb (pure, L)} \rightleftarrows \text{Rb (in Rb–Pb, L)}.$$

The EMF, E, can be written as

$$E = -(RT/F)\ln \gamma_{\text{Rb}} - (RT/F)\ln X_{\text{Rb}} \quad (1)$$

where F is the Faraday constant, R is the universal gas constant, T is the absolute temperature in K, and γ_{Rb} and X_{Rb} are the activity coefficient and atom fraction of rubidium, respectively.

† Callery Chemical Co, Callery, PA 16024, USA.

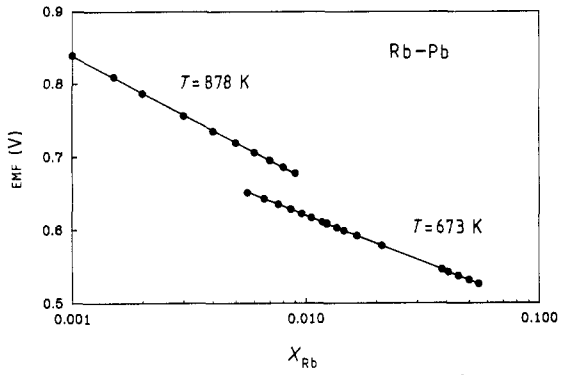

Figure 1. Nernst plots for dilute solutions of Rb–Pb alloys at 673 K and 878 K. The points refer to measurements and the straight lines to the calculated theoretical slopes.

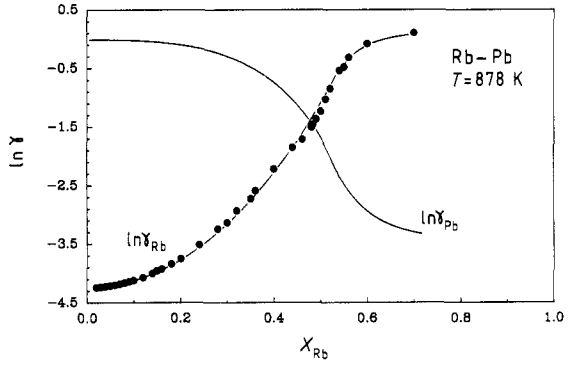

Figure 2. Variation of ln γ as a function of composition at 878 K. The points refer to experiments; full curve for ln γ_{Rb} is fitted by eye to the measurements, while for ln γ_{Pb} it is calculated from the Gibbs–Duhem relation.

For dilute solutions, equation (1) can be simplified to

$$E = E^0_{Rb(Pb)} - (RT/F) \ln X_{Rb} \tag{2}$$

where $E^0_{Rb(Pb)}$ represents the limiting standard potential of Rb in molten lead extrapolated to $X_{Pb} = 1$. Nernst plots at 878 K and 673 K, as expressed by equation (2), are given in figure 1. Linear regression analysis for the Nernst plots gave correlation coefficients of almost unity for all cases. The calculated slopes are in agreement with the theoretical values ($-RT/F$); for example, at 673 K the theoretical slope is $-RT/F = -57.993$ mV compared with the experimental one of -55.010 mV, and at 878 K the theoretical and calculated slopes are -75.658 mV and -73.504 mV respectively. Values for $E^0_{Rb(Pb)}$ are 367.09 mV and 330.57 mV at 673 K and 878 K respectively. There are no values in the literature with which the present results can be compared. However, compared with K–Pb where Saboungi *et al* [7] determined $E^0_{K(Pb)} = 394$ mV at 640 K, $E^0_{Rb(Pb)}$ has slightly lower values.

As the Rb content increases beyond a few atomic per cent, deviations from the Nernst law become significant. For each alloy composition, the Rb activity coefficient can be calculated from equation (1). The Pb activity coefficients are calculated by means of the Gibbs–Duhem integration. Figure 2 shows the variation of ln γ for both components as a function of composition at 878 K. There is an inflection point in the values of ln γ_{Rb} at approximately the equiatomic composition. Furthermore, the rubidium in solution behaves almost ideally at values of $X_{Rb} \geqslant 0.6$ with only slight

Table 1. Selected EMF values measured at 878.0 K for different cells. E is with respect to a pure Rb reference electrode.

	X_{Rb}	E (mV)	ln γ_{Rb}
Cell No 1	0.0200	616.8	−4.241
	0.0300	585.4	−4.231
	0.0400	562.9	−4.221
	0.0500	545.1	−4.209
	0.0600	530.4	−4.197
	0.0700	517.6	−4.182
	0.0800	505.9	−4.162
	0.0900	495.6	−4.142
	0.1000	486.0	−4.121
	0.1500	442.6	−3.953
	0.2001	405.3	−3.749
	0.3001	328.2	−3.135
	0.3500	285.6	−2.725
	0.4000	237.1	−2.217
	0.4400	202.1	−1.851
	0.4800	169.5	−1.506
	0.5000	145.7	−1.233
	0.5500	81.4	−0.479
	0.6000	44.9	−0.083
	0.7001	19.4	+0.101
Cell No 2	0.1000	486.5	−4.128
	0.1200	468.4	−4.071
	0.1400	451.7	−4.004
	0.1600	435.8	−3.927
	0.1800	420.2	−3.839
	0.2000	404.8	−3.741
	0.2400	373.8	−3.514
	0.2800	341.8	−3.245
	0.3200	308.1	−2.933
	0.3600	273.0	−2.586
	0.4000	238.2	−2.233
	0.4400	205.1	−1.890
	0.4600	188.3	−1.712
	0.4832	165.7	−1.462
	0.4900	157.5	−1.368
	0.5000	143.4	−1.202
	0.5100	128.5	−1.025
	0.5200	113.4	−0.845
	0.5400	87.3	−0.538
	0.5600	67.8	−0.316

positive deviations from ideality. Table 1 gives the values of EMF with respect to the pure rubidium reference and the Rb activity coefficients.

The limiting slope, ε, is defined as

$$\varepsilon = (\partial \ln \gamma_{Rb}/\partial X_{Rb})_{X_{Rb}\to 0}. \tag{3}$$

Positive values for ε were derived, ranging from 3 at 673 K to 1 at 878 K. This is much smaller than the value of 5 ± 1 reported for K–Pb [7] and almost identical to that reported

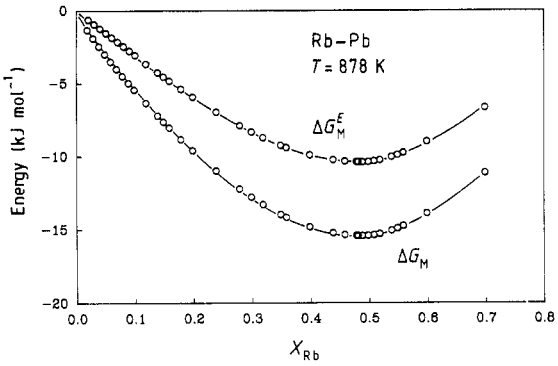

Figure 3. Variations of the Gibbs energy and the excess Gibbs energy of mixing with composition at 878 K.

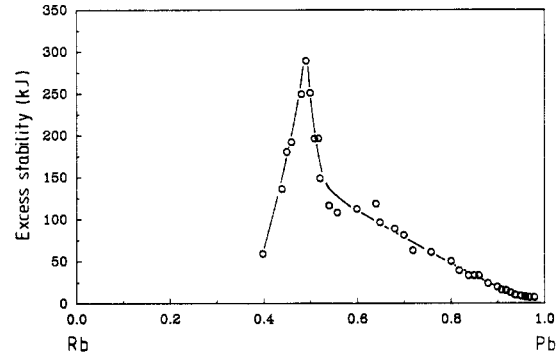

Figure 4. Variations of the Darken excess stability function with composition at 878 K.

for Na–Pb, i.e. 3.6 [4]. The positive sign for the limiting slope indicates an attraction between the unlike atoms and a relative repulsion between like atoms [13].

The integral Gibbs energy of mixing, ΔG_M, and the excess Gibbs energy of mixing, ΔG_M^E, can be calculated from the activity coefficients by means of the following equations:

$$\Delta G_M^E = RT(1 - X_{Rb}) \int_0^{X_{Rb}} \frac{\ln \gamma_{Rb}}{(1 - X'_{Rb})^2} \, dX'_{Rb} \tag{4}$$

$$\Delta G_M = \Delta G_M^E + RT(X_{Rb} \ln X_{Rb} + X_{Pb} \ln X_{Pb}). \tag{5}$$

The variations of the integral and excess Gibbs energies with composition are represented in figure 3. The curves are very nearly symmetrical with a broad minimum about the equiatomic composition, as was the case for the other alkali–lead alloys with the exception of Li–Pb.

A function that is perhaps more indicative of the nature of a solution is the Darken excess stability, defined as

$$ES = \left(\frac{\partial^2 \Delta G_M^E}{\partial X_{Rb}^2}\right)_{P,T} = \frac{RT}{(1 - X_{Rb})} \left(\frac{\partial \ln \gamma_{Rb}}{\partial X_{Rb}}\right)_{P,T}. \tag{6}$$

Note that the ES can be evaluated accurately from the present measurements since it is related to the first derivative of isothermal EMFs. As illustrated in figure 4, the ES has a

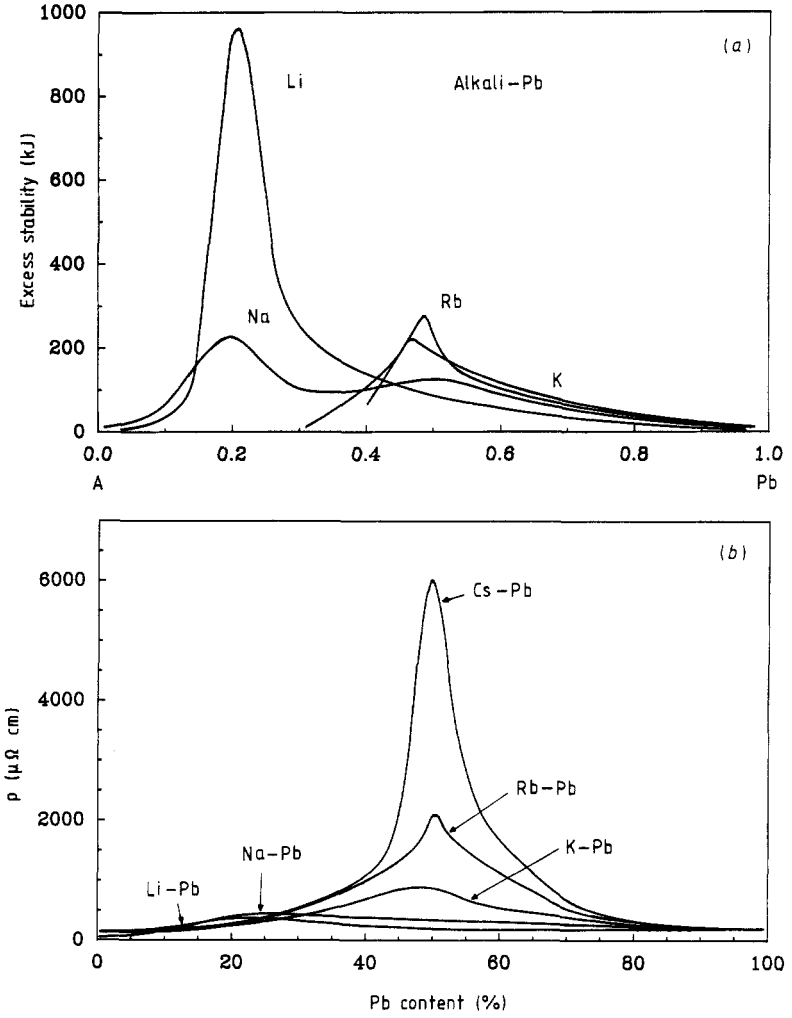

Figure 5. Variations (*a*) of the Darken excess stability functions and (*b*) the electrical resistivities [10, 11] for the Li–Pb, Na–Pb, K–Pb and Rb–Pb systems.

single peak of 289 kJ very near 50 at.% Rb compared with a value of 240 kJ for K–Pb near 50 at.% K. A peak at A_4Pb was observed in the Na–Pb and Li–Pb systems. Two peaks were observed in the Na–Pb system. Figure 5(*a*) is a collection of ES functions of the A–Pb systems (A = Li, Na, K, Rb). Electrical resistivities collected from the literature [10, 11] are plotted in figure 5(*b*). Clearly, the resistivities for Rb–Pb and K–Pb exhibit sharp maxima at approximately the equiatomic composition. Thermodynamic functions can be related to structural functions when such structural functions can be described by a collection of partial structure factors in wave vector space. Bhatia and Thornton [14] described such a situation where the concentration correlation function $S_{CC}(k)$ equals $N\langle\Delta X^2\rangle$ at $k = 0$, where N is the number of atoms and $\langle\Delta X^2\rangle$ is the mean square of the concentration fluctuations in a binary system. Accordingly, it can be shown that

Table 2. Coefficients derived from a numerical treatment of the EMFs collected for different compositions, according to $E(\mathrm{V}) = a + bT\ (°\mathrm{C}) + cT^2\ (°\mathrm{C})$. MCC refers to the multiple correlation coefficient. The coefficients are given to a higher degree of accuracy than the experimental data in order to reproduce the measurements.†

X_{Rb}	a (V)	$10^4 b$ (V °C^{-1})	$10^7 c$ (V °C^{-2})	MCC
0.1000	0.5420	−2.2957	2.2107	0.9935
0.1500	0.5094	−1.9515	1.4006	0.9997
0.2001	0.5038	−2.9441	2.1763	0.9995
0.3001	0.4633	−3.5772	2.2218	0.9999
0.3500	0.4448	−3.8372	1.9917	0.9995
0.4000	0.7133	−13.5665	9.4143	0.9895
0.4400	0.8590	−18.8305	13.2072	0.9936
0.4800	1.2114	−30.4224	21.8200	0.9921
0.5000	0.6807	−15.2965	10.6661	0.9994
0.5500	−0.2503	9.6935	−6.9579	0.9979
0.6000	−0.0571	2.2272	−0.8944	0.9999
0.7001	−0.0416	1.4104	−0.6657	0.9959

† Measurements obtained in the temperature range from the liquidus temperature to a maximum of 900 K.

$$N\langle(\Delta X)^2\rangle = RT(\partial^2 \Delta G_M/\partial X^2)^{-1}.$$

When $k = 0$, the expression for $S_{CC}(k = 0)$ can be derived as

$$S_{CC}(k = 0) = N\langle(\Delta X)^2\rangle = X_{Rb}(1 - X_{Rb})/[X_{Rb}(\partial \ln \gamma_{Rb}/\partial X_{Rb}) + 1]. \quad (7)$$

Accordingly, a maximum in ES will have a corresponding minimum in $S_{CC}(0)$.

3.2. Temperature dependence of the EMFs, entropies, and heat capacities

Experiments were performed at constant composition to determine the temperature dependence of the EMF. For each composition of the Rb–Pb alloy, the EMFs have been fitted to a quadratic expression of the form

$$E\,(\mathrm{mV}) = a + bT + cT^2.$$

The coefficients a, b, and c, as well as the multiple correlation coefficients, are reported in table 2 and results are plotted in figure 6. Note that these measurements were made by decreasing and increasing the temperature.

The entropy functions are calculated using the coefficients of table 2 and the following relations:

$$S^E_{Rb} = F(\partial E/\partial T)_{X,P} + R \ln X_{Rb} \quad (8)$$

$$\Delta S^E_M = (1 - X_{Rb}) \int_0^{X_{Rb}} \frac{S^E_{Rb}}{(1 - X'_{Rb})^2}\, \mathrm{d}X'_{Rb} \quad (9)$$

$$\Delta S_M = \Delta S^E_M - R(X_{Rb} \ln X_{Rb} + X_{Pb} \ln X_{Pb}). \quad (10)$$

The slope of S^E_{Rb} versus X_{Rb} changes abruptly between $X_{Rb} = 0.50$ and 0.55. Consequently, there are pronounced minima in ΔS_M, shown in figure 7, and S^E, which have

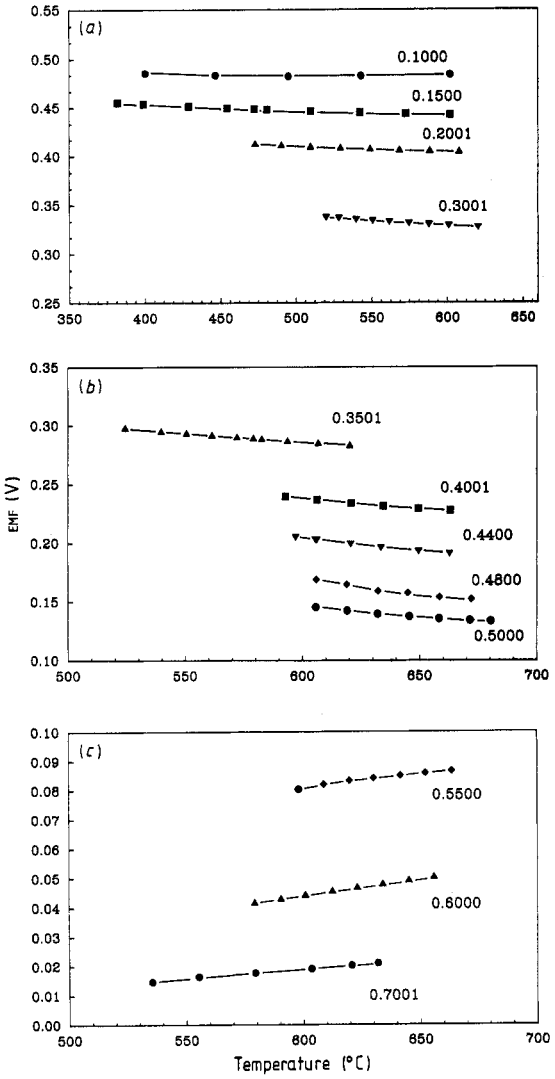

Figure 6. Variations of EMF with temperature for selected alloy compositions, X_{Rb}, given against the curves.

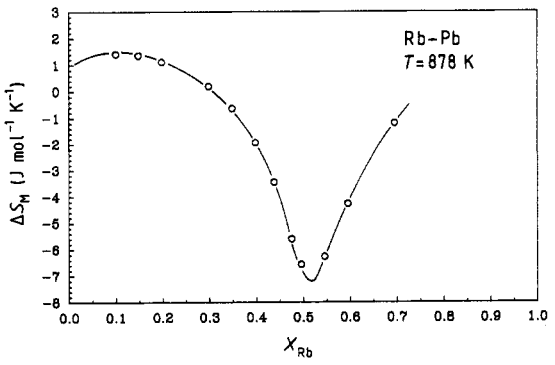

Figure 7. Variations at 878 K of the total entropy of mixing of the Rb–Pb system.

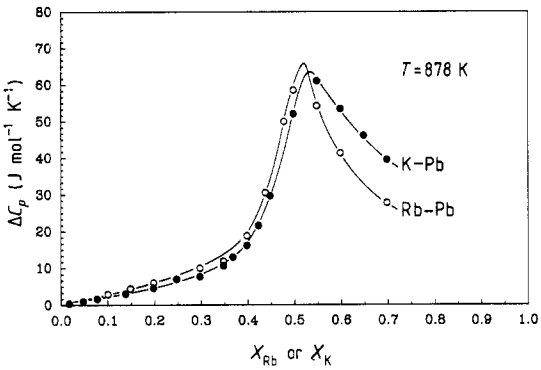

Figure 8. Variations of the average excess heat capacity of K–Pb [7] and Rb–Pb alloys.

Table 3. Values of the excess heat capacity in Rb–Pb alloys at an average temperature of 878 K.

X_{Rb}	ΔC_p (J mol^{-1} K^{-1})
0.1000	3.0
0.1500	4.5
0.2001	6.0
0.3001	10.0
0.3500	11.8
0.4000	18.8
0.4400	30.5
0.4800	50.0
0.5000	58.5
0.5500	54.2
0.6000	41.4
0.7001	27.8

the V-shape typical of ordered systems. The minima are located at approximately 50 at.% Rb. The values of ΔS_M and S^E at this composition are very negative.

The excess heat capacity, ΔC_p, is derived from the EMF measurements as

$$\Delta C_p = C_p - X_{Pb}C^0_{p,Pb} - X_{Rb}C^0_{p,Rb} \tag{11}$$

$$\Delta C_p = T\left(\frac{\partial \Delta S_M}{\partial T}\right) = (1 - X_{Rb})\int_0^{X_{Rb}} \frac{FT(\partial^2 E/\partial T^2)}{(1 - X_{Rb})^2}\, dX'_{Rb} \tag{12}$$

where C_p is the molar heat capacity of the Rb–Pb alloy, $C^0_{p,i}$ is the molar heat capacity of the ith component, and ΔC_p represents the deviation of the heat capacity from additive behaviour. The variations of ΔC_p with composition are given in figure 8; the numerical values grouped in table 3 have a maximum uncertainty of ±20%. As in the K–Pb system, the heat capacity of the Rb–Pb system has a large peak at $X_{Rb} \simeq 50$ at.%. The large values of ΔC_p for compositions near $X_{Rb} = 0.50$ are related to the deviations from linear behaviour in the EMF–temperature curves of figure 6. It should also be noted that the present results for ΔC_p provide an averaged description of the function because the temperature interval over which the second derivative is calculated is small. Recent calorimetric measurements [9] of the heat capacity of liquid equiatomic Rb–Pb agree satisfactorily with the present results. For example, at the equiatomic composition, EMF

results yield $\Delta C_p = 58.50$ J mol^{-1} K^{-1}, to be compared with 50 J mol^{-1} K^{-1} derived from the calorimetric results. As mentioned in the introduction, the interpretation of the behaviour of the alkali–lead alloys is still a challenge. Recent neutron diffraction investigations [15, 16] of the structure of equiatomic APb (A = Na, K, Rb, and Cs) revealed the presence of a sharp diffraction peak at low wave vector ($Q \simeq 1$ Å^{-1}), which is a signature for intermediate range ordering. The large heat capacity peak at the equiatomic composition suggests the presence of ordered structural units that dissociate upon heating, or, at least of an ordered solution that becomes less ordered at higher temperatures. An explanation has been advanced [15, 16] to account for the electrical, thermodynamic, and structural properties based on the formation of a polyvalently charged anion, Pb_4^{4-}, similar to the Zintl ion known to exist in crystalline APb. On these grounds, the heat capacity peak, as well as temperature dependence of the heat capacity, was explained via a dissociation scheme, e.g.

$$A_4Pb_4 \rightleftarrows 4A + 4Pb.$$

The relative abundance of the structural unit A_4Pb_4 and the free atoms A and Pb could then be evaluated from ΔC_p and other information. Thus, the increase in temperature led to an increase in the dissociation of the structural unit. Qualitatively, such a dissociation scheme offers a plausible interpretation. Indeed, at the equiatomic composition, it is reasonable to assume that these structural units prevail; as more alkali metal or lead is added, these units become diluted. This is in consonance with the structural behaviour where the magnitude of the first diffraction peak decreases as the composition of the alloy departs from the 50 : 50 case.

Several thermodynamic models are available in the literature where 'associated' species are considered to explain extreme behaviour, such as peaks in excess stabilities. Although these models could be viewed as providing a 'best' fit for the measured activities and activity coefficients, they fail to reproduce the temperature and composition dependence of the heat capacity. More sophisticated models are needed to account for diverse interactions occurring in these solutions. The available models are suitable only when a 'small' excess heat capacity has been observed as for Na–Cd and Na–In [17] and Na–Pb [3]. The electronic disorder model introduced by Wagner [18] was applied to KPb [19]; it was successful in correlating the measured EMFs and the electrical resistivity, but could not represent the heat capacity. Recently, the stability of anion clusters in several alkali–lead alloys was studied taking into account an electronic charge transfer from the alkali metal to the metalloid [20]. Calculations based on this model are being carried out to explain the anomalous behaviour of the heat capacities.

4. Conclusions

The thermodynamic properties of liquid Rb–Pb alloys show dramatic features that include a large negative entropy of mixing, a pronounced peak in the Darken excess stability function, and a large maximum in the excess heat capacity. A self-consistent interpretation is qualitatively advanced, based on a dissociation of structural units into others and/or into free atoms. The structural units are constructed assuming that the Zintl ion, Pb_4^{4-}, survives the melting process. This assumption is justified by structural and electrical resistivity results. It is hoped that sophisticated thermodynamic models be developed to provide an adequate interpretation of these anomalies.

Acknowledgments

This work was performed at Argonne National Laboratory and supported by the US Department of Energy, Division of Materials Sciences, Office of Basic Energy Sciences, under Contract W-31-109-ENG-38.

References

[1] Demidov A L, Morachevskii A G and Gerasimenko L N 1973 *Elektrokhimiya* **9** 848
[2] Saboungi M-L, Marr J and Blander M 1978 *J. Chem. Phys.* **68** 1375
[3] Matsunaga S, Ishiguro T and Tamaki S 1983 *J. Phys. F: Met. Phys.* **13** 587
[4] Saboungi M-L, Herron S J and Kumar R 1985 *Ber. Bunsenges. Phys. Chem.* **89** 375
[5] Iwase M, Sugino S, Ichise E and Waseda Y 1984 *High-Temp. Mater. Proc.* **6** 143
[6] Maiorova A E, Morachevskii A G and Busse-Machukas V B 1980 *Zh. Prikl. Khim.* **53** 2191
[7] Saboungi M-L, Leonard S R and Ellefson J 1986 *J. Chem. Phys.* **85** 6072
[8] Johnson G K and Saboungi M-L 1987 *J. Chem. Phys.* **86** 6376
[9] Saboungi M-L, Reijers H T J, Blander M and Johnson G K 1988 *J. Chem. Phys.* **89** 5869
[10] Meijer J A, Geertsma W and van der Lugt W 1985 *J. Phys. F: Met. Phys.* **15** 899
van der Marel C, van Oosten A B, Geertsma W and van der Lugt W 1982 *J. Phys. F: Met. Phys.* **12** 2349
[11] Meijer J A 1988 *PhD Thesis,* Groningen University, Netherlands
Meijer J A, van der Lugt W and Vinke G J B 1986 *J. Phys. F: Met. Phys.* **16** 845
[12] Petric A, Pelton A D and Saboungi M-L 1988 *J. Electrochem. Soc.* **135** 2754
[13] Saboungi M-L and Corbin T P 1984 *J. Phys. F: Met. Phys.* **14** 13
[14] Bhatia A B and Thornton D E 1970 *Phys. Rev.* A **2** 3004
[15] Saboungi M-L, Blomquist R, Volin K J and Price D L 1987 *J. Chem. Phys.* **87** 2278
[16] Reijers H T J, Saboungi M-L, Price D L, Richardson J W Jr, Volin K J and van der Lugt W 1989 *Phys. Rev.* B **40** 698
[17] Harada S, Takahashi S, Takeda S, Tamaki S, Gray P and Cusack N E 1988 *J. Phys. F: Met. Phys.* **18** 2559
[18] Wagner C 1977 *Progress in Solid State Chemistry* vol 6, ed H Reiss and J O McCaldin (New York: Pergamon)
[19] Saboungi M-L, Leonard S R, Johnson G K and Price D L 1989 *Alloy Phase Stabililty, NATO ASI Series E: Applied Sciences* vol 163 ed. G M Stocks and A Gonis (Kluwer: Dordrecht) p 627
[20] Geertsma W 1989 private communication